JOURNAL OF Applied Polymer SCIENCE

Elongational Flow Mixing for Manufacturing of Graphite Nanoplatelet/Polystyrene Composites

Henrik Oxfall,[1] Jérôme Rondin,[2] Michel Bouquey,[2] René Muller,[2] Mikael Rigdahl,[1] Rodney W. Rychwalski[1]

[1]Department of Materials and Manufacturing Technology, Chalmers University of Technology, S-41296 Göteborg, Sweden
[2]Group for the Intensification and Intrapolation of Polymer Processes (G2IP), Laboratory of Polymer Engineering for High Technologies (LIPHT), European Engineering School of Chemistry, Polymer, and Material Science (ECPM), University of Strasbourg (UdS), 25 Rue Becquerel, F-67000 Strasbourg, France
Correspondence to: H. Oxfall (E-mail: henrik.oxfall@chalmers.se)

ABSTRACT: Manufacturing strategy is of prime importance for the appropriate incorporation of filler into a polymeric matrix, and this in particular refers to nanofillers. Herein, direct-graphite nanoplatelets are used as filler in polystyrene. The as-received filler material contained microscopic size agglomerates formed by nanoscopic size graphite nanoplatelets. Refining of the microagglomerates (break-up) and production of, desirably, single graphene layers (exfoliation) is the ultimate target for controlling production and thus properties of the present materials. Several processing methods including microcompounding, roll-milling/calendering, Brabender mixing chamber, and solvent processing are used and compared with elongational flow mixing by a newly developed mixer. For the present system, sonication with surfactant assistance solvent processing yields both good micro deagglomeration and production of thin graphene nanostacks/layers. Also the elongational flow mixing efficiently refines the microagglomerates. Solvent processing and microcompounding are more efficient than the other processes in the production of exfoliated thin graphene stacks/layers. © 2012 Wiley Periodicals, Inc. J. Appl. Polym. Sci. 000: 000–000, 2012

KEYWORDS: polystyrene; rheology; nanotubes; grapheme; fullerenes

Received 27 March 2012; accepted 6 August 2012; published online
DOI: 10.1002/app.38439

INTRODUCTION

Graphene-based fillers are on the one hand creating a wealth of new opportunities, and on the other hand also questions for their use in polymer matrices. Their technological application is far from being fully understood and established. Experience with a similar disruptive technology, carbon nanotubes (CNT), shows that carbon nanoparticles may efficiently impart desirable behavior to polymers, for example electroactivity, like electrical conductivity, piezoelectricity, photorefractivity, and others.[1–4] Similarly, it may be expected that graphene-based polymer nanocomposites will be among the fastest growing applications of graphene.[5] Properties and applications of graphene-based polymer nanocomposites have been overviewed recently, for example by Kim et al.,[6] Potts et al.,[7] and Sengupta et al.[8]

It is well known that the quality of polymer nanocomposites first of all hinges on the quality of the filler and its incorporation into the polymer matrix. In a study recently, we focused on refining of direct-graphite nanoplatelets (GNP) by solvent dispersion, and incorporation of thin graphene stacks obtained by exfoliating the nanoplatelets, into polystyrene (PS) matrix.[9] In the present report we will focus on manufacturing aspects alleviating preparation of GNP/PS by melt processing. We will use a newly developed melt elongational flow dispersive mixing (EFDM) instrument.

Dispersive mixing conditions are determined by the balance between the integrity (cohesive forces holding agglomerates/aggregates or droplets together) and the disruptive hydrodynamic forces. Since the pioneering work by Taylor,[10] followed by several other studies for example,[11–13] the elongation and break-up of droplets and particles in elongational flow, have been studied. It has been demonstrated that elongational flow enhances the process of deagglomeration, compared with shear flow.[14,15] Recently, several research works have further focused on EFDM, and on mixing devices to efficiently realize the flow. The present state of the equipment development has been overviewed by Bouquey et al.[16] Herein, we employ a newly developed elongational flow reactor and mixer[16] to compound graphite nanoparticles with polystyrene. Consequently, the obtained nanocomposites are

compared with those prepared using other melt processing techniques, and also using solvent processing.

Graphene-based polymer nanocomposites with PS as matrix material have been studied earlier. Abdel-Goad et al., as well as Li and Chen, used melt mixing,[17,18] Stankovich et al., Goyal et al., and Liu et al. used solvent mixing,[19–21] Chen et al. used *in situ* polymerization,[22] and Tkalya et al. used latex-based process.[23] Several groups have carried out research into graphene-based nanocomposites using other polymer matrices, where melt mixing and solvent-based mixing have been compared, for example.[24–27] Results from these studies show that solvent-based mixing is a more efficient technique to deagglomerate and disperse GNP. In Ref. 18, the authors used roll milling to produce masterbatches consisting of high density polyethylene (HDPE) or PS with expanded graphite (EG). Composites prepared from the masterbach by a melt extrusion process showed better dispersion and lower percolation threshold compared to the ones prepared directly in the extruder. Also Zhan et al. have shown that composites prepared via a masterbatch route results in lower percolation threshold.[28]

A common important consideration in using GNP as filler in polymers is the resulting electrical conductivity. At the percolation threshold, the conductivity of the composite starts increasing rapidly. The critical content at which the electrical percolation onsets in graphene-based polymer nanocomposites ranges from as low as 0.1 vol % filler[21] to about 20 wt %[18] depending on matrix material, filler, and mixing method.

Graphite and graphite oxide (GO) are important alternative sources enabling at present preparation of GPNC where massive amounts of filler are needed. Graphite nanoparticles used in this work have been developed and studied by Drzal and coworkers.[24,26,29–33] The advantage of graphite nanoparticles, in contrast to GO, is that the π-orbital structure of graphene is not disrupted due to oxidation, and the electrical conductivity of the filler is not worsened. Indeed, the oxides can be reduced (by thermal or chemical reduction) resulting in increased electrical conductivity, however, the reduction step adds to the processing chain. Thus we used GNP in the present work.

There are numerous challenges to be dealt with in the present study, and the two main ones are: (i) the availability and suitability at present of graphene/graphite nanoparticles for high quality polymer nanocomposites for electrical applications, and (ii) efficient and practical refining of graphite nanoparticles during manufacturing, and the impact on electrical properties. It is the purpose of this study to particularly focus on the use of elongational flow processing to achieve micro- and nanoscopic refinement of graphite nanoplatelets and compare results, with other processing methods, with a high-voltage application of the nanocomposites in mind.

EXPERIMENTAL

Materials

The polymer used is a commercial grade of polystyrene, Polystyrol 143 E, from BASF, Germany, with a density of 1043 kgm^{-3} and a melt volume rate (200°C, 5 kg) of 10 cm^3/10 min. The graphite nanoparticles used are xGnP, from XG Sciences, USA, with a thickness between 1 and 15 nm, average thickness of 5 nm, and an average diameter of 5 μm, as given by the producer.

Table I. Elongational Flow Compounding: Processing Options

Processing option/ sample	Filler content (wt %)	Piston speed (mm s^{-1})	Number of cycles	Mixing time (s)	Mixing energy (J g^{-1})
F1	5	16	10	144	163
F2	5	16	20	240	272
F3	5	16	40	336	380
F4	5	31.2	10	103	169
F5	5	31.2	20	172	281
F6	5	31.2	40	240	395
F7	10	18.7	10	163	206
F8	10	18.7	20	272	343
F9	10	18.7	40	380	480
F10	10	27.1	10	112	210
F11	10	27.1	20	186	350
F12	10	27.1	40	261	490

Preparation

Composites containing 0, 5, 10, 15, and 20 wt % GNP were prepared to map the nanocomposite filler content dependence. Subsequently, the 5 and 10 wt % compositions were again manufactured using the compounding methods, with typical processing parameters, described below.

Mixing Chamber. Brabender mixing chamber, with a volume of 50 cm^3 was used. The mixing was done at 200°C at 100 rpm for 10 min. The Brabender mixed composite was used as the starting material in the three following melt preparations.

Elongational Flow Compounding. Elongational flow reactor and mixer (RMX, Scamex) were used. Description of the compounder is given in Ref. 16. This recently built device realizes flow between two opposite chambers through a small diameter die. The material is alternately pushed from one chamber to the other through the die. Thus convergent and divergent elongational flow takes place at the entrance and exit of the die, contributing to dispersive mixing. In comparison with existing laboratory mixers, the flow in the present mixer is characterized by a high contribution from elongational flow. The mixing die used had a length of 28 mm and a diameter of 2 mm and a processing temperature of 200°C was used. Two different piston speeds, one high and one low, was used and materials were collected after 10, 20, and 40 cycles, see Table I. The pressure inside the chamber and the displacement of the piston were recorded and the mixing energies could be calculated, as shown elsewhere.[16]

High Shear Energy Microcompounding. Haake Micro Compounder (Rheomex CTW5) twin screw microcompounder with corotating screws was used. The materials were mixed at 100 rpm for 7 min at 200°C.

Roll Milling/Calendering. A 2-roll mill (Polymix 150 P Schwabenthan) was used. The definition of roll milling in contrast to calendering may vary in practice, but a ratio of roll radius to nip of 200–500 for calenders and that of 30–60 for mills, is frequently used as the criterion. The present equipment uses mills of radius 75 mm. The nip was continuously reduced from the initial value of 2–0.1 mm, during a processing run, implying respectively milling (initial processing) and calendering (final processing). Rolls were rotating at the same speed of 10 rpm, temperature was 200°C, and mixing time was 6 min.

Solvent Mixing. *N*-methyl-pyrrolidone (NMP), Merck, and nonionic surfactant Triton X-100, Alfa Aesar, were used. PS and NMP, 1:15 wt concentration, were stirred at room temperature until the polymer was completely dissolved after 2 h. Pristine GNP was mixed together with NMP, 1:20 wt concentration. Triton X-100 was added to NMP, 1:200 wt concentration. The mixture was first stirred for 15 min, and then sonicated for 2 h in a Branson 1510 E-MTH bath (70 W), Branson Ultrasonic. After sonication, the GNP-NMP-Triton mixture was added to PS-NMP mixture and stirred for 30 min followed by additional sonication for 2 h. In all sonication steps, the temperature did not exceed ~ 60°C. After sonication, the mixture was stirred again for 10 min, a subset sample was removed and transferred to a vial for sedimentation observations, and the main mass of liquid was poured into wide glass bowls to let the solvent evaporate at 55°C during 24 h. Finally, the material was dried in vacuum oven at 80°C during 48 h.

Rheological Measurements

Stress controlled rotational rheometer, Rheometrics SR200, was used at 200°C under N_2 atmosphere. Compression molded samples with a diameter of 25 mm and a thickness of 2 mm were fitted into a parallel plate fixture. A dynamic time sweep was conducted at 0.5 Hz using a low stress until stabilization of the storage modulus G' was observed, as suggested by.[34,35] This took 600–2400 s, depending on material. Dynamic stress sweeps, to determine the linear viscoelastic region, and dynamic frequency sweeps were conducted after G' had stabilized. The frequency sweeps were conducted within the linear viscoelastic region.

Microscopy and Image Analysis

Leitz DMXR optical microscope (OM), Germany, was used to evaluate the deagglomeration of graphite particles in composites containing 5 wt % GNP. Extrudates, with a diameter of 1 mm, produced in a capillary rheometer were mounted in a polymeric resin in such a way that the cross section of the extrudates could be examined. The mounted extrudates were then polished with 9, 3 and finally 1 μm diamond paste to achieve a smooth mirror like surface of the sample. Finally images of the polished surface were produced at a magnification of 100 times and Axio Vision, release 4.7.2, imaging system was used to perform image analysis.

Zeiss EM912 Omega electron transmission microscope (TEM) equipped with Ω energy filter and operated at 120 keV was used to study thin graphene nanoplatelets deposited onto holey carbon grids (400 mesh).

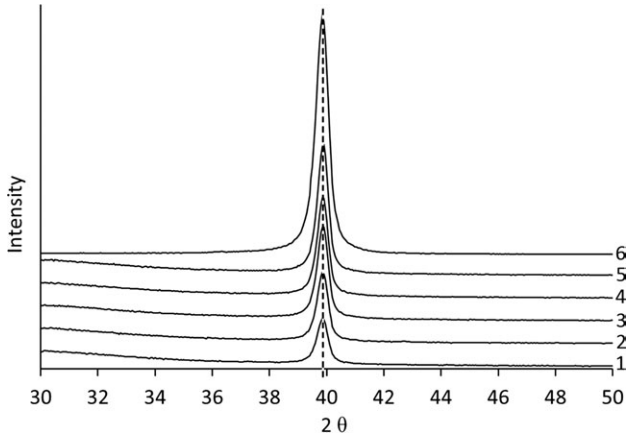

Figure 1. X-ray diffractograms for composites containing 5 wt % GNP prepared with different mixing methods: (1) solvent processing, (2) elongational flow (F6), (3) roll milling, (4) Brabender mixing chamber, (5) Haake microcompounder, (6) pure GNP.

Electrical Conductivity

Keithley 6517 A electrometer equipped with a Keithly 8009 resistivity test fixture was used to measure volume resistivity on compression molded samples with a diameter of 80 mm and a thickness of 1 mm. The resistivity test fixture uses a three-terminal method, where an extra guard electrode is applied around the sample to avoid measurement errors due to leakage currents. An applied voltage between 1 and 10 V was used during the measurements depending on the conductivity of the composites. The surface of the plates was roughened to ensure good contact of filler with the electrodes. The experimental scatter is about ±7%, based on measurements on an individual specimen. All measurements were carried out at room temperature and relative humidity of 30% ± 5%.

X-Ray Diffraction

X-ray diffractograms (XRD) were obtained using a Siemens D8 Advanced Thetra X-ray diffractometer. The radiation source was a Cr Kα with a wavelength of 2.28970 Å. An increase of 0.05° every 5 s was used and the sample was rotating with a speed of 30 rpm. Measurements were performed at room temperature on circular discs with a diameter of 25 mm, and a thickness of ~ 2 mm.

RESULTS AND DISCUSSION

Morphological

In the following, microscopic and nanoscopic material structure is discussed. The microscopic analysis matches the size of nanoplatelet (in-plane dimensions) and that of the agglomerates of nanoplatelets. The nanoscopic analysis matches the nanoplatelet thickness. It turns out that filler particle refinement on both, nanoscopic and microscopic scales, can take place during manufacturing, and the refinement depends on the manufacturing method. For all mixing methods, as was observed from XRD diffractograms, GNP was not fully exfoliated and not intercalated. This was evident from the diffraction peak always present and always at the same angle, 39.8°, as can be seen in Figure 1.

In high-voltage applications, large agglomerates can result in an inhomogeneous electric field and could thus be detrimental for

Applied Polymer SCIENCE

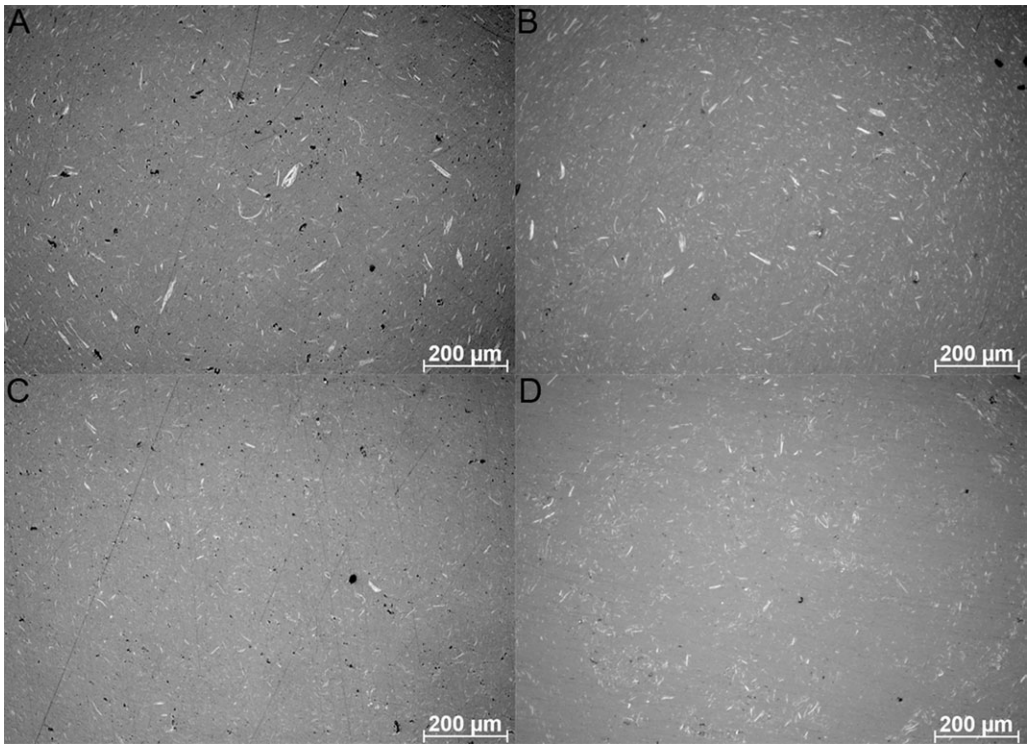

Figure 2. OM images of typical microscopic morphologies resulting from different manufacturing methods: (A) Brabender mixing chamber, (B) Haake microcompounder, (C) RMX compounder, (D) solvent-based preparation. A 5 wt % GNP was used in all cases.

material stability. In Figure 2, typical microscopic morphologies resulting from different manufacturing methods are shown. Good light transparency of PS matrix facilitates imaging and both filler particles on the surface and somewhat below are seen, and appear white since the filler particles reflects light, while the matrix appears grey. Black spots are voids (not included in the following image analysis). In this work we have used optical microscopy to evaluate the amount of large agglomerates present in the composites. Large agglomerates are highly undesirable in the material for at least two reasons: (i) they increase the electrical percolation threshold and, (ii) as mentioned earlier they reduce the electrical stability in a high voltage application.

Image analysis results are given in Figures 3 and 4. To ensure representative results, 9 images of typically 100 microagglomerates per image were analyzed. Agglomerates with an area of $<50\ \mu m^2$ were not included in the analysis due to the difficulty in accurately identifying them in the Axio Vision imaging system. In the histograms in Figures 3 and 4, the microagglomerate size is represented by the sectional area contribution (area fraction) within ranges (μm^2) 50–100 (small agglomerates), 100–250 (intermediate size), and >250 (large agglomerates). In Figure 3, the different manufacturing methods are represented.

As shown in Figure 3, the smallest amount of large microagglomerates and simultaneously the largest amount of small microagglomerates are produced in the composite manufactured by elongational flow mixing using processing option F6. A close morphology is measured for the solvent prepared material. Both manufacturing methods give much higher microdispersibility compared to the other manufacturing methods for the present system and experimental parameters. Similarly, in Figure 4, by comparing various processing options used in elongational flow mixing, it is seen that the processing options with the highest mixing energies (F6 and F3) provide highest microdispersibility quality (mixing energy is given in Table I).

The microdispersibility imparted by microcompounding is lower than that by elongational flow mixing, and is higher than that by Brabender mixing chamber processing and two-roll milling/calendering. It is remarkable that high microscopic

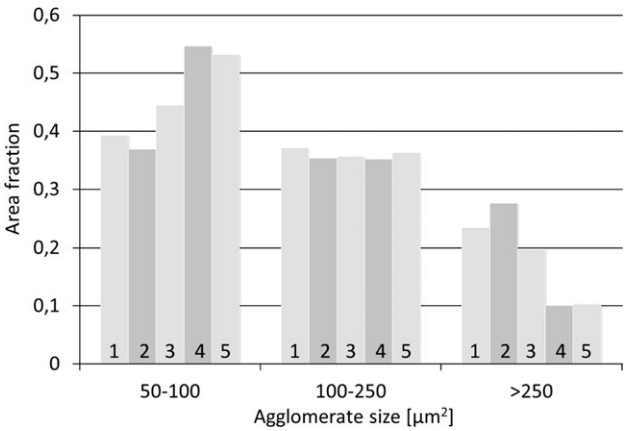

Figure 3. Histogram representing various manufacturing methods employed to prepare the 5 wt % composition: (1) mixing chamber, (2) roll milling, (3) microcompounder, (4) elongational flow (F6), (5) solvent processing.

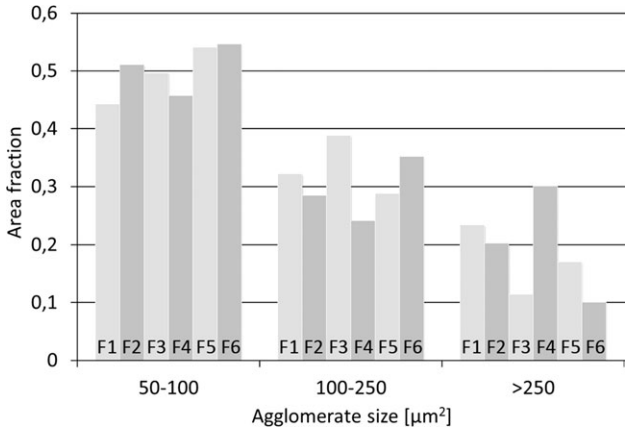

Figure 4. Histogram representing processing options F1-F6 used in the elongational flow mixing applied to the 5 wt % composition.

dispersibility of GNP in PS, practically the same as in solvent processing, can be obtained by melt processing when elongational flow mixing is employed.

Surface area per volume of flake-shaped filler strongly increases at high aspect ratios. Clearly, exfoliated graphene layers have high aspect ratio and surface area. However, agglomeration of graphene leads to a dramatic loss of the ultrahigh surface area, say from well above 2000 m^2g^{-1} to $\sim$ 40 m^2g^{-1} for stacks.[36] Partly overlapping layers of shifted graphene can build up the stack length. The high surface area and aspect ratio are commonly accepted as translating to ability of particle bridging and electrical conductivity. Electron passage may take place by contact and/or by tunneling effect, the latter when the distance between conducting domains becomes sufficiently small (there is no entire agreement in the literature as to the required distance, and the lowest published values are $\sim$ <5 nm.[37–39])

Thus, exfoliation of graphite is important for efficient imparting of electrical conductivity, and methods are being recently developed to exfoliate graphite.[40–43] Herein, we used a procedure (see Solvent Mixing section) developed by us to bulk separate thin graphene stacks from initially thicker graphite nanoplatelets. Details of the method are given elsewhere[9]; graphene stacks consisting mainly of three layers, not more than five layers, are formed. A TEM image of graphene layers using our solvent exfoliation method is shown in Figure 5.

In Figure 5, three graphene layers (short arrows) partly overlapping, can be observed. The dark shade of grayscale/black color (long arrow), and the architecture thereabout may be interpreted as rolled (or folded) graphene sheet corner, with an increased amount of polymer molecules. This condition is believed to lower the electrical conductivity enhancement[44]; however, it may just be the opposite when bridging between layers of aligned graphene sheets enables off-plane connectivity.

Rheological Properties

We further analyze filler connectivity/networking by means of rheological characteristics. In general, networking for rheological and electrical effects, are not strictly the same. The critical filler concentration for electrical percolation is slightly higher than that for rheological one, which is usually explained by different requirement for minimum proximity in the two cases, being smaller in the case of electrical percolation.[7] On the other hand, since rheological properties are measured in the molten state, and the volume expansion of the polymer is greater than that of the GNP, the higher temperature will result in filler volume content decrease. Still, the rheological percolation approach is helpful and is increasingly used to gain insight into particle networking. It has the advantage compared to TEM observations, that it is nonlocal. In the rheological approach, the storage or loss shear modulus, G' or G'', or their combination, are analyzed. Frequency dependence of G' and G'' for a range of nanocomposites containing 0–20 wt % filler initially mixed in the Brabender mixing chamber, and then microcompounded, are shown in Figure 6(A, B), respectively. We preferred to analyze G', taking into account that the effect on G' in the case of anisometric fillers, is more pronounced,[45] which can clearly be seen in Figure 6.

As well known, networking of filler is manifested by the apparent yield stress seen as a plateau at low frequencies, for example.[6] This can be seen in Figure 6(A), starting from 5 wt % filler content, and increasingly taking place at higher filler contents. Therefore, interconnected graphite particles can be assumed to be present in the composite, increasingly dominating the behavior with the increasing filler concentration. At high concentrations of graphite nanoplatelets, networking is more pronounced imparting a higher stiffness (G' value). At low filler concentrations, G' is lower than G'' at low frequencies (<1 Hz). However, at 15 wt % filler $G' = G''$ is observed at low frequencies. The crossover point is sometimes interpreted in percolation terms in the literature.[46]

In Figure 7(G') as a function of frequency measured on nanocomposites (5 and 10 wt %) processed using various manufacturing methods, are shown.

In Figure 7(A), mechanical filler networking takes place in the case of solvent-processed material, where flattening out of the plot at lower frequencies is seen. Less clearly, weak flattening

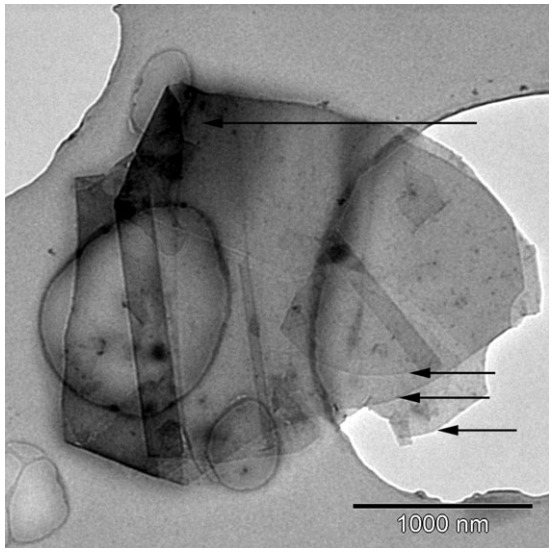

Figure 5. TEM image showing graphene layers.

Applied Polymer SCIENCE

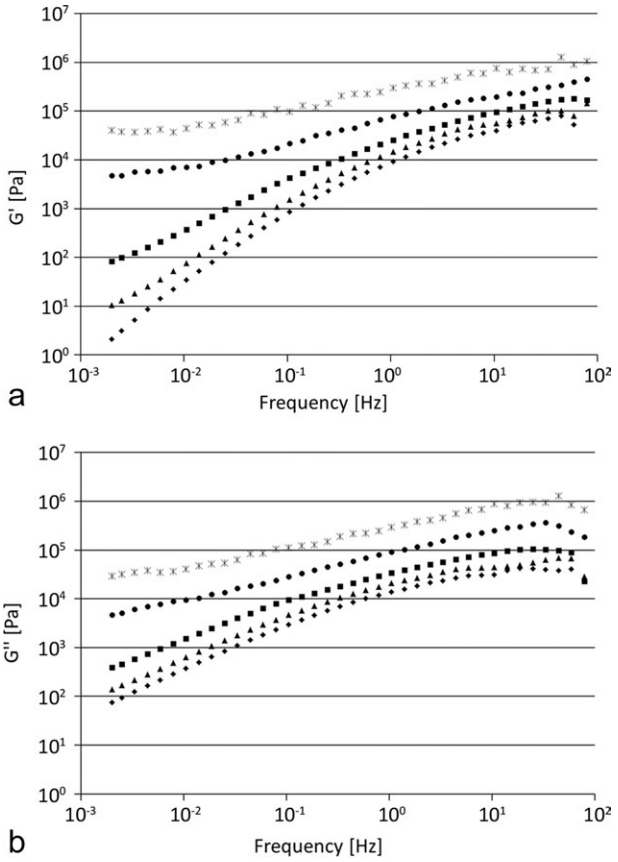

Figure 6. (A) G' vs. frequency, (B) G'' vs. frequency, for a range of nanocomposites containing 0–20 wt % filler initially mixed in the Brabender mixing chamber, and then microcompounded: (◆) PS, (▲) 5 wt %, (■) 10 wt %, (●) 15 wt %, (x) 20 wt %.

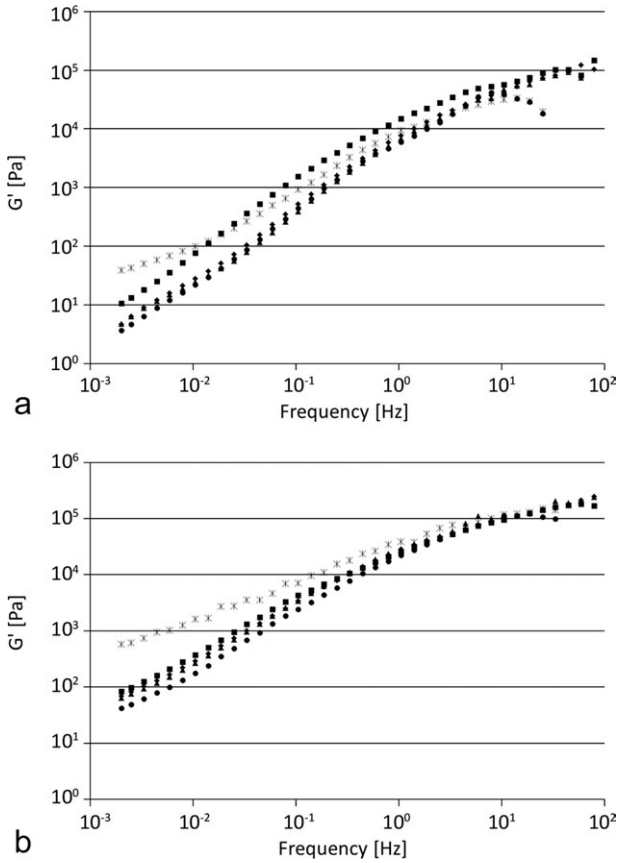

Figure 7. G' vs. frequency of materials processed using various manufacturing methods: (A) 5 wt %, (B) 10 wt %: (◆) mixing chamber, (▲) roll milling, (■) microcompounder, (●) elongational flow (F6), (x) solvent processing.

out at low frequencies takes place also in the case of microcompounding. In Figure 7(B), all plots flatten out at lower frequencies, the difference being that the inflection point takes place at different frequencies, e.g., at the highest frequency in the case of solvent processing. The nearest to this behavior is shown by the microcompounded material. In other words, the plateau behavior spreads out over a wider or narrower frequency range, depending on the manufacturing method. Finally, we note that on the whole the plots at 10 wt % concentration are flatter (less stiffness increase with the increasing frequency) than those at 5 wt % concentration. Thus, depending on the manufacturing method, in several cases, and to a varying degree, flattening out of G' plots takes place. This behavior will be related to electrical conductivity results, ahead.

$\acute{G}$ data represent melt stiffness. As can be expected, all 10 wt % materials have higher stiffness. Interestingly, for each of the concentrations, the melt stiffness is lower during elongational flow and roll-milling compounding, compared to the remaining processes, which can be an advantage.

Electrical Conductivity

Electrical conductivity results are summarized in Table II, where also the applied voltage used during the measurements can be noted.

At 5 wt % concentration of filler, all composites have reached the electrical percolation. For all the melt processed materials the percolation threshold is just below 5 wt % and the materials are very weakly statically dissipative with a volume conductivity

Table II. Electrical Conductivity of Materials Manufactured Using Various Methods

Manufacturing method	Filler content (wt %)	Volume conductivity (S cm^{-1})	Applied voltage (V)
Mixing chamber	5	1.21E−10	10
	10	4.39E−07	5
Roll milling	5	8.77E−11	10
	10	1.13E−06	5
Micro compounder	5	1.44E−10	10
	10	4.12E−06	5
Elongational flow	5 (F6)	1.10E−10	10
	10 (F12)	1.15E−06	5
Solvent processing	5	1.06E−06	5
	10	1.06E−05	1
Unfilled material (PS)	0	4.38E−17	400

close to 1×10^{-10} S cm^{-1}. The solvent processed material has a percolation threshold well below 5 wt % and the conductivity is 1.06×10^{-6} S cm^{-1}, and thus is fairly semiconductive. The electrical conductivity of solvent processed-material is much higher compared to other manufacturing methods.

At 10 wt %, material conductivity ranges from 4.39×10^{-7} to 1.06×10^{-5} S cm^{-1}. The solvent-processed material is still the most conductive but the increase in conductivity from 5 wt % is much less compared to the melt-processed materials. We explain this by conductivity approaching a plateau value above the percolation threshold. Comparing melt-processed materials at 10 wt %; the microcompounded material is slightly more conductive compared to other manufacturing methods.

Electrical conductivity results well reconcile with the rheological results, and both can be explained in manufacturing terms. Solvent processing is more efficient in production of exfoliated graphene layers, compared to melt processing, and the increased amount of graphene layers imparts higher networking within the filler, and consequently the conductivity. At 5 wt %, where the average distance between the microagglomerates is larger than at 10 wt %, the presence of graphene layers is particularly critical. Here, the solvent processed material contains exfoliated layers enabling filler connectivity (observed as the rheological plateau), offering highest conductivity. At 10 wt %, microagglomerates are closer one to each other, and thus the role of the graphene layers is less dramatic; connectivity can take place on the microscopic level in all materials, as can be judged from the rheological plots. All 10 wt % materials have increased conductivity compared to 5 wt %. The highest conductivity of the solvent-processed material can be understood from the higher amount of exfoliated layers. The next highest conductivity takes place in the microcompounded material. We explain this by shear flow exfoliation, where graphene layers can be peeled apart from graphite. This mechanism was proposed by Paul and Robeson[47] for layered silicates in shear flow during melt processing. At 10 wt %, materials manufactured by elongational flow and roll-milling/calendering have slightly lower conductivity. We ascribe this to lower exfoliation ability of the two processes. The lesser connectivity is represented in the rheological plots as less developed plateau.

CONCLUSIONS

A recently developed elongational flow reactor and mixer was used to compound graphite nanoplatelets with polystyrene. Comparisons were made with traditional melt mixing techniques using typical processing parameters (microcompounding, roll-milling/calendering, and Brabender mixing chamber), and with sonication and surfactant assisted solvent processing. Not surprisingly it is found that solvent processing is the most efficient dispersive mixing technique for imparting electrical conductivity, particularly feasible at lower filler content. GNP microagglomerates break-up, and formation of thin graphene stacks takes place. The elongational flow mixer equally efficiently breaks up GNP microagglomerates compared to solvent based mixing, and more efficiently than the other melt mixing techniques, for the present system. The improved microrefinement found in the present case of polystyrene matrix is promising, and can be expected to take place in other matrices of use for preparing high quality nanocomposites, for high-voltage applications. Nanocomposites manufactured with the use of elongational flow mixer did not show though lower electrical percolation threshold. Microcompounding was found to be the most efficient melt mixing technique with respect to imparting electrical conductivity. Again, as was for solvent processing, exfoliation is crucial. Because of shear flow during microcompounding, graphene stacks/layers are likely to be more efficiently peeled apart from graphite imparting particle connectivity playing a role in electron mobility.

ACKNOWLEDGMENTS

The authors thank Bin Ma at the Department of Materials and Manufacturing Technology, Chalmers University of Technology, for the help with electrical measurements, Christer Svanberg, Borealis AB, for discussions, and Urban Jelvestam, Department of Materials and Manufacturing Technology, Chalmers University of Technology, for the help with XRD measurements. The financial support from the Swedish Foundation for Strategic Research (SSF) is acknowledged.

REFERENCES

1. Sandler, J. K. W.; Kirk, J. E.; Kinloch, I.A.; Shaffer, M. S. P.; Windle, A. H. *Polymer* **2003,** *44*, 5893.
2. Martin, C. A.; Sandler J. K. W.; Shaffer, M. S. P.; Schwarz M.-K.; Bauhofer, W.; Schulte, K.; Windle, A. H. *Compos. Sci. Technol.* **2004,** *64*, 2309.
3. Lund, A.; Gustafsson, C.; Bertilsson, H.; Rychwalski, R. W. *Compos. Sci. Technol.* **2011,** *71*, 222.
4. Vannikov, A. V.; Grishina, A. D.; Rychwalski, R. W. *Carbon* **2011,** *49*, 311.
5. Tassinari, O.; Bradley, J.; Grosse, J.; Holman, M. *Lux Res. Rep.* **2009,** LRNI-R-09-001.
6. Kim, H.; Abdala, A. A.; Macosko, C. W. *Macromolecules.* **2010,** *43*, 6515.
7. Potts, J. R.; Dreyer, D. R.; Bielawski, C. W.; Ruoff, R. S. *Polymer.* **2011,** *52*, 5.
8. Sengupta, R.; Bhattacharya, M.; Bandyopadhyay, S.; Bhowmick, A. K. *Prog. Polym. Sci.* **2011,** *36*, 638.
9. Persson, H.; Yao, Y.; Klement, U.; Rychwalski, R. W. *Express Polym. Lett.* **2012,** *6*, 142.
10. Taylor, G. I. *Proc. R Soc. Lond. Ser A.* **1932,** *138*, 41.
11. Powell, R. L.; Mason, S. G. *AlChE J.* **1982,** *28*, 286.
12. Min, K.; White, J. L.; Fellers, J. F. *J. Appl. Polym. Sci.* **1984,** *29*, 2117.
13. Manas-Zloczower, I.; Feke, D. L. *Int. Polym. Proc.* **1989,** *4*, 3.
14. Macosko, C. W. Rheology Principles, Measurements, and Applications; VCH Publishers: New York, **1994;** Chapter 7, p 285.
15. Tadmor, Z. G.; Gogos, C. G. Principles of Polymer Processing; Wiley-Interscience: New York, **1979;** Chapter 11, p 434.

16. Bouquey, M.; Loux, C.; Muller, R.; Bouchet, G. *J. Appl. Polym. Sci.* **2010,** *119*, 482.
17. Abdel-Goad, M.; Pötschke, P.; Zhou, D.; Mark J. E.; Heinrich, G. *J. Macromol. Sci. A Pure Appl. Chem.* **2007,** *44*, 591.
18. Li, Y. C.; Chen, G. H. *Polym. Eng. Sci.* **2007,** *47*, 882.
19. Stankovich, S.; Dikin, D. A.; Dommett, G. H. B.; Kohlhaas, K. M.; Zimney, E. J.; Stach, E. A.; Pinter, R. D.; Nguyen, S. T.; Ruoff, R. S. *Nature* **2006,** *442*, 282.
20. Goyal, R. K.; Jagadale, P. A.; Mulik, U. P. *J. Appl. Polym. Sci.* **2009,** *111*, 2071.
21. Liu, N.; Luo, F.; Wu, H.; Liu, Y.; Zhang, C.; Chen, J. *Adv. Funct. Mater.* **2008,** *18*, 1518.
22. Chen, G.; Wu, C.; Weng, W.; Wu, D.; Yan, W. *Polymer.* **2003,** *44*, 1781.
23. Tkalya, E.; Ghislandi, M.; Alekseev, A.; Koning, C.; Loos, J. *J. Mater. Chem.* **2010,** *20*, 3035.
24. Kalaitzidou, K.; Fukushima, H.; Drzal, L. T. *Compos. Sci. Technol.* **2007,** *67*, 2045.
25. Shen, J. W.; Chen, X. M.; Huang, W. Y. *J. Appl. Polym. Sci.* **2003,** *88*, 1864.
26. Kim, S.; Do, I.; Drzal, L. T. *Macromol. Mater. Eng.* **2009,** *294*, 196.
27. Kim, H.; Macosko, C. W. *ANTEC* **2009,** *1*, 122.
28. Zhan, Y.; Lei, Y.; Meng, F.; Zhong, J.; Zhao, R.; Liu, X. *J. Mater. Sci.* **2011,** *46*, 824.
29. Kalaitzidou, K.; Fukushima, H.; Drzal, L. T. *Compos. A.* **2007,** *38*, 1675.
30. Kalaitzidou, K.; Fukushima, H.; Drzal, L. T. *Carbon* **2007,** *45*, 1446.
31. Kalaitzidou, K.; Fukushima, H.; Askeland, P.; Drzal, L. T. *J. Mater. Sci.* **2008,** *43*, 2895.
32. Kim, S.; Seo, J.; Drzal, L. T. *Compos. A.* **2009,** *41*, 581.
33. Kim, S.; Drzal, L. T. *J. Adhes. Sci. Technol.* **2009,** *23*, 1623.
34. Kim, H.; Macosko, C. W. *Polymer* **2009,** *50*, 3797.
35. Kim, H.; Macosko, C. W. *Macromolecules* **2008,** *41*, 3317.
36. Si, Y.; Samulski, E. T. *Chem. Mater.* **2008,** *20*, 6792.
37. Pötschke, P.; Abdel-Goad, M.; Pegel, S.; Jehnichen, D.; Mark, J. E.; Zhou, D.; Heinrich, G. *J. Macromol. Sci. A Pure Appl. Chem.* **2010,** *47*, 12.
38. Rittigstein, P.; Priestley, R. D.; Broadbelt, L. J.; Torkelson, J. M. *Nat. Mater.* **2007,** *6*, 278.
39. Du, F.; Scogna, R. C.; Zhou, W.; Brand, S.; Fischer, J. E.; Winey, K. I. *Macromolecules* **2004,** *37*, 9048.
40. Khan, U.; O'Neill, A.; Lotya, M.; De, S.; Coleman, J. N. *Small* **2010,** *6*, 864.
41. Green, A. A.; Hersam, M. C. *Nano Lett.* **2009,** *9*, 4031.
42. Bourlinos, A. B.; Georgakilas, V.; Zboril, R.; Sterioti, T. A.; Stubos, A. K. *Small* **2009,** 5, 1841.
43. Blake, P.; Brimicombe, P. D.; Nair, R. R.; Booth, T. J.; Jiang, D.; Schedin, F.; Ponomarenko, L. A.; Morozov, S. V.; Gleeson, H. F.; Hill, E. W.; Geim, A. K.; Novoselov, K. S. *Nano Lett.* **2008,** *8*, 1704.
44. Yi, Y. B.; Tawerghi, E. *Phys. Rev. E Stat. Nonlinear Soft Matter. Phys.* **2009,** *79*, 041134.
45. Utracki, L. A. *Polym. Compos.* **1986,** *7*, 274.
46. Kotsilkova, R. Thermoset Nanocomposites for Engineering Applications; Smithers Rapra Technology Limited: Shawbury, **2007;** Chapter 2, p 25.
47. Paul, D. R.; Robeson, L. M. *Polymer.* **2008,** *49*, 3187.